Supporting Information for

Fe-Substituted $Na_{3.5}V_{1.5}Mn_{0.5}(PO_4)_3$ NaSICON Cathode with Multi-Electron Reactions and Improved Energy Output

Loubna Chayal[a], Soraia El Moutchou[b], Noha Sabi[b], Hicham Ben Youcef[b], Hasna Aziam[b,*], Mohamed Saadi[a], and Mohammed Hadouchi[a,*]

[a]*Laboratoire de Chimie Appliquée des Matériaux, Centre des Sciences des Matériaux, Faculty of Science, Mohammed V University in Rabat, Avenue Ibn Battouta, BP 1014, Rabat, Morocco*

[b]*High Throughput Multidisciplinary Research (HTMR), College of Chemical Sciences and Engineering (CCSE), Mohammed VI Polytechnic University (UM6P), Lot 660 Hay Moulay Rachid, Ben Guerir, 43150, Morocco*

*Corresponding authors:

Hasna Aziam: Hasna.AZIAM@um6p.ma and Mohammed Hadouchi : m.hadouchi@um5r.ac.ma

Note S1. Raman-based determination of lateral crystallite size (L_a):

The lateral crystallite size (La) was determined from the I_{D1}/I_G ratio using the Tuinstra-Koenig relation:

$$L_a = \frac{4.4}{\frac{I_{D1}}{I_G}} \times \left(\frac{2.41}{E_L}\right)^4 \quad \textbf{(S1)}$$

where E_L represent the laser energy, which is equal to 2.3308 eV for 532 nm.

Note S2. Theoretical Capacity:

The theoretical capacity ($C_{theoretical}$) of $Na_{3.5}V_{1.5}Mn_{0.25}Fe_{0.25}(PO_4)_3$ is calculated by the following formula:

$$C_{theoretical} = (n \times F)/(M \times 3.6)$$

Where F is the Faraday constant (96485 C/mol), M is the molecular weight of $Na_{3.5}V_{1.5}Mn_{0.25}F_{0.25}(PO_4)_3$ (469.5 g/mol) and n is the number of electrons (assumed to be 2).

$$C_{theoretical} = (2 \times 96485)/(469.5 \times 3.6)$$

$C_{theoretical}$~114.2 mAh g^{-1}

Note S3. Energy density:

Energy density = Average discharge voltage× discharge capacity of the cathode material

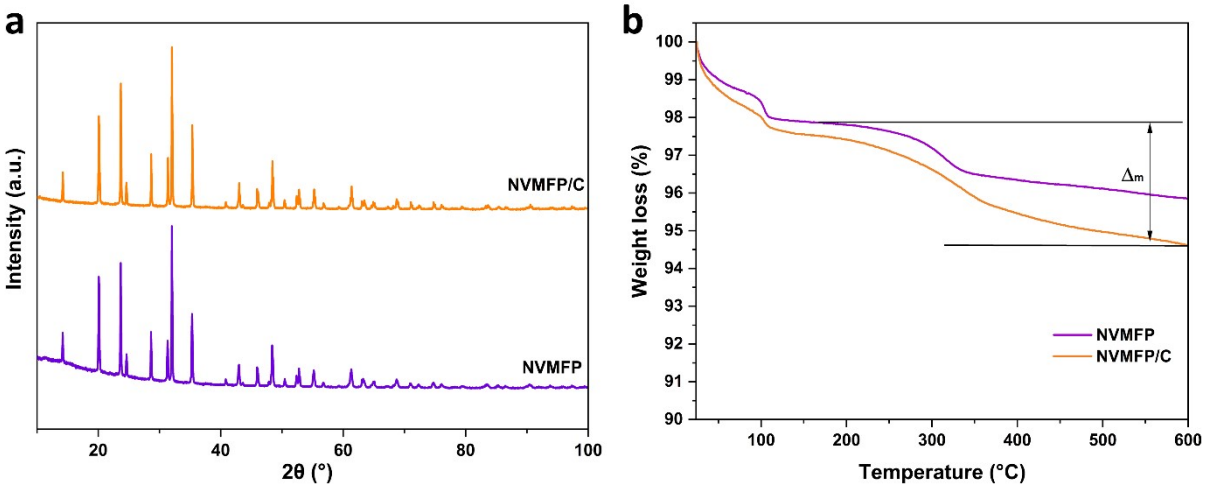

Fig. S1. (a) XRD patterns and **(b)** TG curves of NVMFP and of NVMFP/C powders.

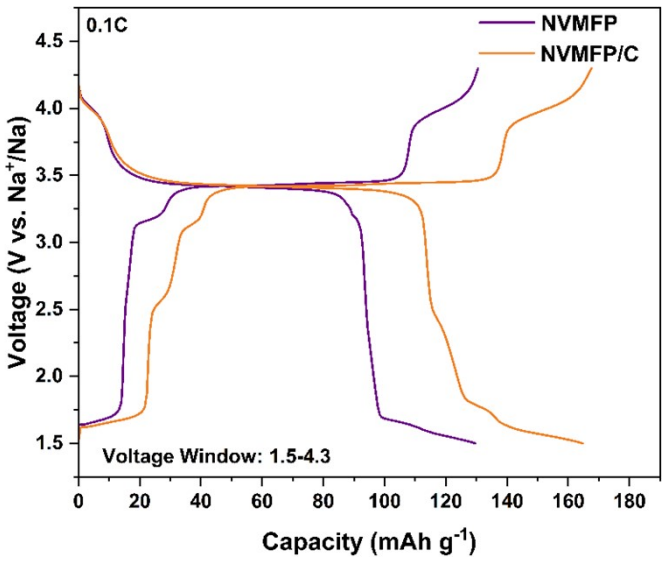

Fig. S2. Second charge–discharge profile of NVMFP and NVMFP/C cathodes at 0.1 C.

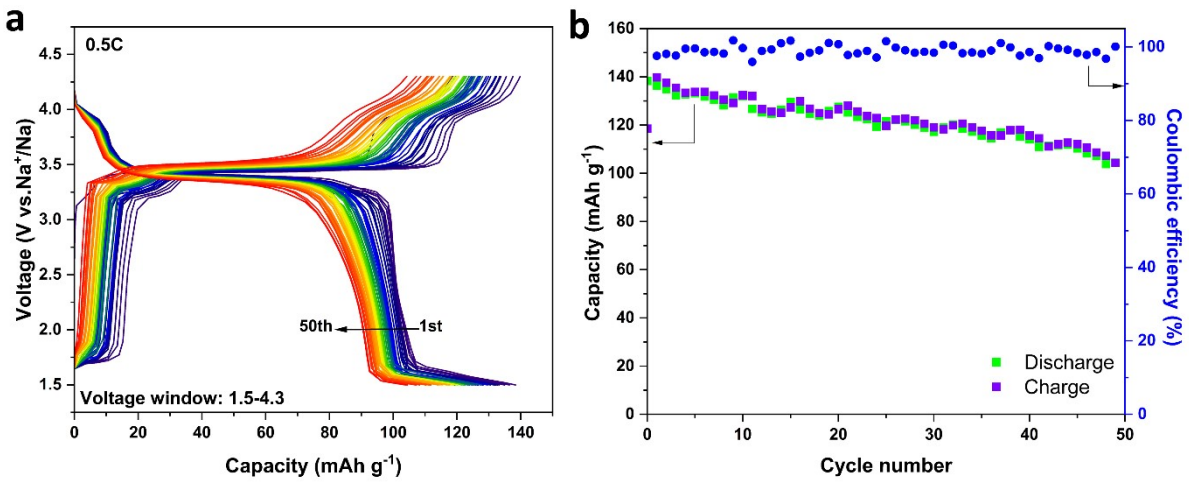

Fig. S3. Cycling performance of NVMFP/C at 0.5 C.

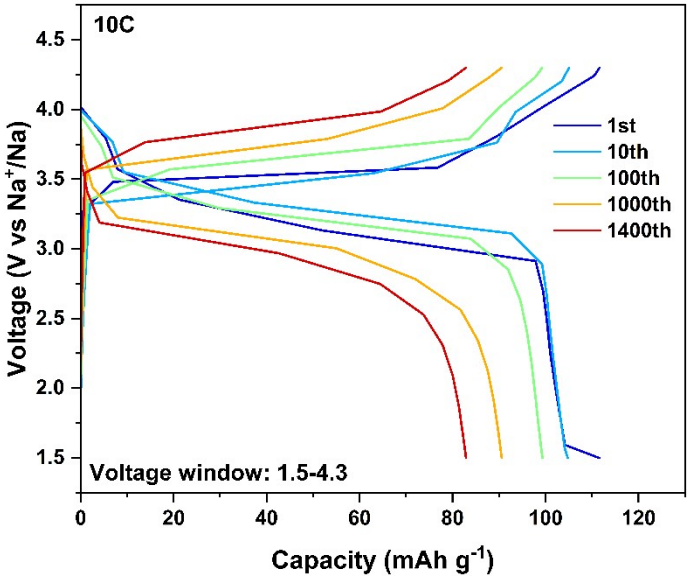

Fig. S4. Voltage profiles of NVMFP/C at 10 C for different cycle numbers.

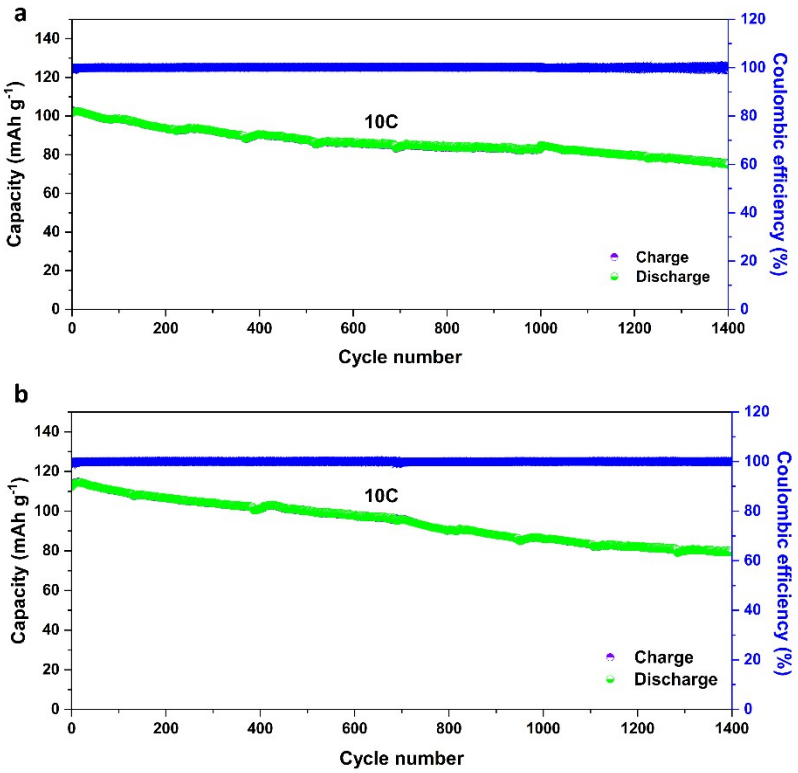

Fig. S5. Repeatability tests of NVMFP/C at 10 C.

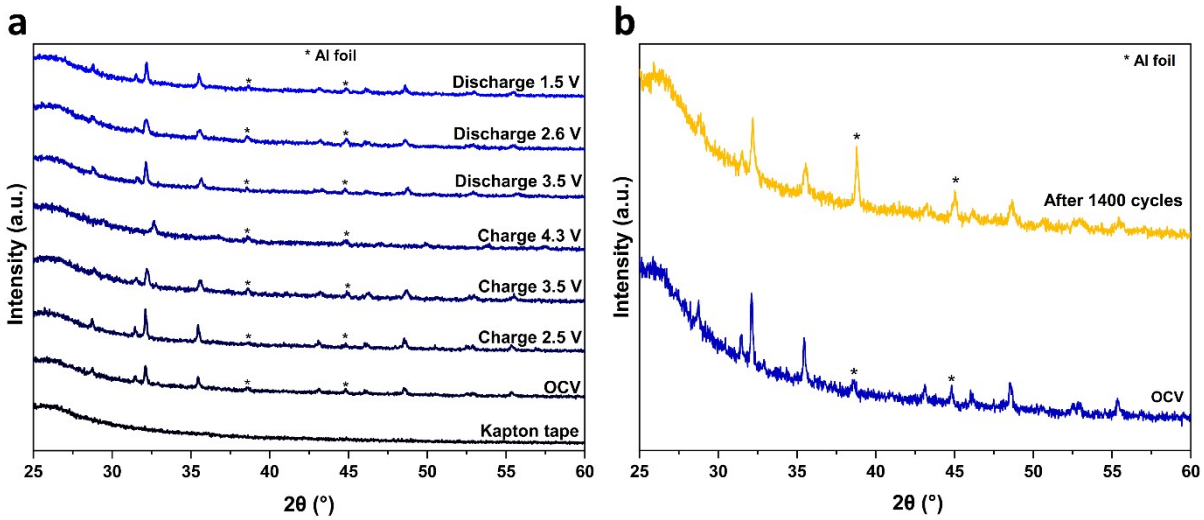

Fig. S6. Ex-situ XRD patterns of NVMFP/C **(a)** at different voltage stages during the first cycle at C/10 and **(b)** after 1400 cycles at 10 C.

Table S1. Elemental composition of Na, Mn, and Fe in the NVMFP/C sample determined by ICP-OES.

ICP results	Na	Mn	Fe
	3.42	0.26	0.26

Table S2. Geometric parameters (Å, º) for NVMFP/C.

Distances (Å)			
P1—O1^{i}	1.539 (4)	V1—O2	2.005 (5)
P1—O1^{ii}	1.539 (5)	V1—O2^{v}	2.005 (4)
P1—O2^{iii}	1.505 (5)	V1—O2^{iii}	2.005 (6)
P1—O2^{iv}	1.505 (5)	Na1—O1	2.517 (4)
Fe1—O1	2.031 (4)	Na1—O1^{v}	2.517 (5)
Fe1—O1^{v}	2.031 (5)	Na1—O1^{iii}	2.517 (5)
Fe1—O1^{iii}	2.031 (5)	Na1—O1^{vi}	2.517 (4)
Fe1—O2	2.005 (5)	Na1—O1^{vii}	2.517 (5)
Fe1—O2^{v}	2.005 (4)	Na1—O1^{viii}	2.517 (5)
Fe1—O2^{iii}	2.005 (6)	Na2—O1^{i}	2.488 (7)
Mn1—O1	2.031 (4)	Na2—O1^{ix}	2.395 (4)
Mn1—O1^{v}	2.031 (5)	Na2—O1^{ii}	2.488 (6)
Mn1—O1^{iii}	2.031 (5)	Na2—O1^{x}	2.395 (5)
Mn1—O2	2.005 (5)	Na2—O2^{xi}	3.217 (6)
Mn1—O2^{v}	2.005 (4)	Na2—O2^{xii}	2.857 (7)
Mn1—O2^{iii}	2.005 (6)	Na2—O2^{xiii}	3.217 (7)
V1—O1	2.031 (4)	Na2—O2^{xiv}	2.857 (6)
V1—O1^{v}	2.031 (5)	Na2—O2^{i}	2.604 (4)
Angles (º)			
O1^{i}—P1—O1^{ii}	110.1 (4)	O1^{v}—Mn1—O1^{iii}	85.6 (4)
O1^{i}—P1—O2^{iii}	110.4 (4)	O1^{v}—Mn1—O2	87.8 (3)
O1^{i}—P1—O2^{iv}	106.5 (4)	O1^{v}—Mn1—O2^{v}	87.7 (3)
O1^{ii}—P1—O2^{iii}	106.5 (5)	O1^{v}—Mn1—O2^{iii}	171.0 (5)
O1^{ii}—P1—O2^{iv}	110.4 (6)	O1^{iii}—Mn1—O2	171.0 (4)
O2^{iii}—P1—O2^{iv}	113.1 (4)	O1^{iii}—Mn1—O2^{v}	87.8 (3)
O1—Fe1—O1^{v}	85.6 (3)	O1^{iii}—Mn1—O2^{iii}	87.7 (3)
O1—Fe1—O1^{iii}	85.6 (3)	O2—Mn1—O2^{v}	98.1 (3)
O1—Fe1—O2	87.7 (3)	O2—Mn1—O2^{iii}	98.1 (5)
O1—Fe1—O2^{v}	171.0 (4)	O2^{v}—Mn1—O2^{iii}	98.1 (4)
O1—Fe1—O2^{iii}	87.8 (3)	O1—V1—O1^{v}	85.6 (3)
O1^{v}—Fe1—O1^{iii}	85.6 (4)	O1—V1—O1^{iii}	85.6 (3)
O1^{v}—Fe1—O2	87.8 (3)	O1—V1—O2	87.7 (3)
O1^{v}—Fe1—O2^{v}	87.7 (3)	O1—V1—O2^{v}	171.0 (4)
O1^{v}—Fe1—O2^{iii}	171.0 (5)	O1—V1—O2^{iii}	87.8 (3)
O1^{iii}—Fe1—O2	171.0 (4)	O1^{v}—V1—O1^{iii}	85.6 (4)

$O1^{iii}$—Fe1—$O2^{v}$	87.8 (3)	$O1^{v}$—V1—O2	87.8 (3)
$O1^{iii}$—Fe1—$O2^{iii}$	87.7 (3)	$O1^{v}$—V1—$O2^{v}$	87.7 (3)
O2—Fe1—$O2^{v}$	98.1 (3)	$O1^{v}$—V1—$O2^{iii}$	171.0 (5)
O2—Fe1—$O2^{iii}$	98.1 (5)	$O1^{iii}$—V1—O2	171.0 (4)
$O2^{v}$—Fe1—$O2^{iii}$	98.1 (4)	$O1^{iii}$—V1—$O2^{v}$	87.8 (3)
O1—Mn1—$O1^{v}$	85.6 (3)	$O1^{iii}$—V1—$O2^{iii}$	87.7 (3)
O1—Mn1—$O1^{iii}$	85.6 (3)	O2—V1—$O2^{v}$	98.1 (3)
O1—Mn1—O2	87.7 (3)	O2—V1—$O2^{iii}$	98.1 (5)
O1—Mn1—$O2^{v}$	171.0 (4)	$O2^{v}$—V1—$O2^{iii}$	98.1 (4)
O1—Mn1—$O2^{iii}$	87.8 (3)		

Symmetry codes: (i) -x+2/3, -y+1/3, -z+1/3; (ii) -x+y+1/3, y-1/3, z+1/6; (iii) -x+y, -x, z; (iv) y, x, -z+1/2; (v) -y, x-y, z; (vi) -x, -y, -z; (vii) y, -x+y, -z; (viii) x-y, x, -z; (ix) y+2/3, -x+y+1/3, -z+1/3; (x) x+1/3, x-y-1/3, z+1/6; (xi) x+1, y, z; (xii) -y+1, x-y, z; (xiii) x-y+1, -y, -z+1/2; (xiv) -x+1, -x+y, -z+1/2.

Table S3. Raman spectra deconvolution results and I_D/I_G intensity ratios for NVMFP and NVMFP/C samples presented in Fig. 1d.

Sample	Peak	Center Max	Max Height	FWHM	Peak ratio	I_D/I_G
NVMFP	D4	1223.4020	994.8166	75.8727	D4/G	0.4299
	D1	1354.5700	5043.9100	90.6398	D1/G	2.1801
	D3	1544.3270	3772.5240	82.4604	D3/G	1.6357
	G	1609.4750	2313.6230	36.5847	-	-
NVMFP/C	D4	1244.2860	1244.2860	74.1806	D4/G	0.3262
	D1	1357.1150	4692.2040	77.6917	D1/G	1.2303
	D3	1537.0830	4000.7500	98.4868	D3/G	1.0489
	G	1594.7400	3813.9180	36.1320	-	-

Table S4. Performance comparison of some V/Mn/Fe-based polyanionic cathodes.

Cathode	Electrolyte system	Active mass basis (%)	Mass loading (mg cm^{-2})	Voltage window	Voltage (V)	Rate Performance	Capacity retention	Ref.
$Na_{3.25}V_{1.75}Mn_{0.25}(PO_4)_3$@C	1 M $NaClO_4$ in PC:EC (1:1 v/v)	75	2.5	2.7 – 4.2 V	3.38	107.0 mA h g^{-1} at 0.1 C 105.1 mA h g^{-1} at 0.2 C 101.6 mA h g^{-1} at 0.5 C 98.5 mA h g^{-1} at 1 C 95.3 mA h g^{-1} at 2 C 90.8 mA h g^{-1} at 5 C 86.4 mA h g^{-1} at 10 C	82.54% after 500 cycles at 1C	[1]
$Na_4V_{0.8}Al_{0.2}Mn(PO_4)_3$	1 M $NaClO_4$ in PC + 2% FEC	70	5.5	2.5 – 3.8 V	3.47	91.7 mA h g^{-1} at 0.2 C 89.9 mA h g^{-1} at 0.5 C 86.8 mA h g^{-1} at 1 C 86.4 mA h g^{-1} at 2 C 85.5 mA h g^{-1} at 5 C 84.4 mA h g^{-1} at 10 C 83.3 mA h g^{-1} at 20 C 83.1 mA h g^{-1} at 30 C 82.1 mA h g^{-1} at 40 C	92% after 1000 cycles at 5C	[2]
$Na_{3.5}Mn_{0.5}V_{1.5}(PO_4)_3$/C (carbon content of 7.9 wt%)	1 M $NaClO_4$ in PC + 5% FEC	75	1.8	2.5 – 4.1 V	3.43	108.6 mA h g^{-1} at 1 C 108.3 mA h g^{-1} at 2 C 108.3 mA h g^{-1} at 5 C 107.0 mA h g^{-1} at 10	90.7% after 500 cycles at 5C 87.2% after 4000	[3]

						C 104.5 mA h g^{-1} at 20 C 100.1 mA h g^{-1} at 40 C 92.7 mA h g^{-1} at 60 C	cycles at 20 C	
$Na_{3.5}Mn_{0.5}V_{1.5}(PO_4)_3$@C@CNTs	1 M $NaClO_4$ in PC + 10 wt% FEC	70	2.5±0.5	2.5 – 4.2V	3.45	120 mA h g^{-1} at 0.2 C 114.1.4 mA h g^{-1} at 0.5 C 110.8 mA h g^{-1} at 1 C 106.6 mA h g^{-1} at 2 C 101.8 mA h g^{-1} at 5 C 96.2 mA h g^{-1} at 10 C	~80 % after 8000 cycles at 10 C 80.2 % after 2000 cycles at 5C	[4]
$Na_{3.04}V_{1.96}Mn_{0.04}(PO_4)_3$@CNTs	1 M $NaClO_4$ in PC + 2 vol% FEC	70	1.5	2.3 – 4.1 V	3.35	120.8 mA h g^{-1} 0.1 C 112.7 mA h g^{-1} 1 C 105.8 mA h g^{-1} 3 C 102.5 mA h g^{-1} 5 C 98.7 mA h g^{-1} 9 C	68.21% after 4000 cycles at 50 C	[5]
$Na_{3.4}VFe(PO_4)_3$	1 M $NaClO_4$ in EC: DMC + 5 wt.% FEC	70	~0.8-1.2	1.7 – 4.3 V	~2.9	121.21 mA h g^{-1} 0.1 C 100 mA h g^{-1} 0.2 C 77 mA h g^{-1} 0.5 C 70 mA h g^{-1} 1 C 56 mA h g^{-1} 2 C 42.7 mA h g^{-1} 5 C 32.7 mA h g^{-1} 10 C 26.3 mA h g^{-1} 20 C 27.9 mA h g^{-1} 50 C	46% after 500 cycles at 1 C	[6]
$Na_3V_{1.5}Mn_{0.5}(PO_4)_3$	1 M $NaClO_4$ in EC/PC (1:1 v/v) + 2 wt% FEC	70	~1	1.4 – 4.0 V	3.34	155.5 mA h g^{-1} at 1 C 145.4 mA h g^{-1} at 2 C 132.4 mA h g^{-1} at 3 C 114.4 mA h g^{-1} at 5 C 96.0 mA h g^{-1} at 7 C 85.5 mA h g^{-1} at 9 C 79.4 mA h g^{-1} at 10 C	~60% after 300 cycles at 5 C	[7]
$Na_{3.3}V_{1.5}Mn_{0.3}Al_{0.2}(PO_4)_3$	1 M $NaClO_4$ in PC + 2% FEC	70	5	2.5 – 4.2 V	3.44	126.6 mA h g^{-1} at 0.1 C 122.2 mA h g^{-1} at 0.2 C 119.8 mA h g^{-1} at 0.5 C 116.8 mA h g^{-1} at 1 C 115.mA h g^{-1} at 2 C 111 mA h g^{-1} at 5 C 107 mA h g^{-1} at 10 C 94 mA h g^{-1} at 20 C	88.8% after 3000 cycles at 10 C	[8]
$Na_{3.25}VMn_{0.25}Fe_{0.75}(PO_4)_3$/NC@CNTs	1 M $NaClO_4$	80	1.0−1.5	2.0 − 3.8 V	3.14	107.9 mA h g^{-1} at 0.1 C 101.7 mA h g^{-1} at 0.5 C 98.1 mA h g^{-1} at 1 C 86.9 mA h g^{-1} at 5 C 78.9 mA h g^{-1} at 10 C 57.2 mA h g^{-1} at 20 C	80.1% after 2000 cycles at 10 C	[9]
$Na_4VMn_{0.5}Fe_{0.5}(PO_4)_3$	1 M $NaClO_4$ in PC + 2% FEC	70	3.5	2.0 − 3.8 V (Cycling Performance) 2.0 − 4.0V (Rate Performance)	~3	120.0 mA h g^{-1} at 0.5 C 113.6 mA h g^{-1} at 1 C 109.2 mA h g^{-1} at 2 C 106.0 mA h g^{-1} at 5 C 103.1 mA h g^{-1} at 10 C 95.5 mA h g^{-1} at 20 C	99.3% after 500 cycles at 5 C 94% after 3000 cycles at 20 C	[10]
$Na_4VFe(PO_4)_3$	1 M $NaClO_4$ in PC + 5 % FEC	80	-	1.5 − 4.2 V	2.95	154.7 mA h g^{-1} at 0.1 C 126.2 mA h g^{-1} at 0.2 C 117.2 mA h g^{-1} at 1 C 110.0 mA h g^{-1} at 2 C 103.9 mA h g^{-1} at 5 C 98.6 mA h g^{-1} at 10 C 94.3 mA h g^{-1} at 15 C 90.8 mA h g^{-1} at 20 C	80 % after 800 cycles at 20 C	[11]
$Na_{3.5}V_{1.5}Mn_{0.25}Fe_{0.25}(PO_4)_3$	1 M $NaClO_4$ in PC:EC (1:1 v/v) + vol% FEC	70	~2	1.5 − 4.3 V	3.07	146 mA h g^{-1} at 0.5 C 134 mA h g^{-1} at 1 C 119 mA h g^{-1} at 2.5 C 101 mA h g^{-1} at 4 C 97 mA h g^{-1} at 5 C	74.34 % after 1400 cycles at 10 C	This work

Table S5. Fitting quality parameters for b-value determination.

Peak	b-values	Fitting quality metrics	Voltage region (V)
R1	0.50014 ± 0.02682	R-Square (COD) 0.99428 Adj. R-Square 0.99142	2.99-2.86

R2	0.72078 ± 0.04146	R-Square (COD) 0.99343 Adj. R-Square 0.99014	3.27-3.16
R3	0.73449 ± 0.01064	R-Square (COD) 0.99958 Adj. R-Square 0.99937	3.89-3.84
O1	1.0212 ± 0.0321	R-Square (COD) 0.99803 Adj. R-Square 0.99704	3.46-3.33
O2	0.47896 ± 0.02657	R-Square (COD) 0.99388 Adj. R-Square 0.99704	3.86-3.71
O3	0.9354 ± 0.06959	R-Square (COD) 0.98905 Adj. R-Square 0.98358	4.19-4.60

Table S6. Evolution of sodium concentrations for the NVMFP/C cathode during the charging process, including the $D \times t \times L^{-2}$ kinetic condition and associated error bars.

xNa^+ in $Na_xV_{1.5}Fe_{0.25}Mn_{0.25}(PO_4)_3$	D	$D \times t \times L^{-2}$	Error bar
3.42495	3.95762×10^{-12}	6.54152×10^{-4}	15,84%
3.37491	3.20433×10^{-11}	0.0053	5,51%
3.32488	4.89188×10^{-11}	0.00809	5,97%
3.27484	4.23901×10^{-11}	0.00701	6,32%
3.2248	2.51344×10^{-11}	0.00415	5,16%
3.17476	5.82855×10^{-11}	0.00963	17,11%
3.12471	1.18132×10^{-10}	0.01953	18,24%
3.07467	9.36868×10^{-11}	0.01549	37,25%
3.02463	1.71616×10^{-10}	0.02837	45,76%
2.97459	1.00391×10^{-10}	0.01659	25,11%
2.92455	1.07628×10^{-10}	0.01779	28,73%
2.87452	7.64607×10^{-11}	0.01264	10,39%
2.82448	4.64958×10^{-11}	0.00769	8,62%
2.77445	9.46162×10^{-11}	0.01564	8,76%
2.72441	1.84933×10^{-10}	0.03057	7,98%
2.67437	1.69126×10^{-10}	0.02795	9,21%
2.62433	1.27717×10^{-10}	0.02111	10,30%
2.57429	6.69881×10^{-11}	0.01107	7,13%
2.52426	5.8116×10^{-11}	0.00961	6,04%
2.47422	9.61848×10^{-11}	0.0159	7,36%
2.42419	7.98018×10^{-11}	0.01319	5,84%
2.37415	7.40489×10^{-11}	0.01224	10,98%
2.32411	7.89045×10^{-11}	0.01304	8,89%
2.27407	7.54975×10^{-11}	0.01248	9,90%
2.22403	9.41466×10^{-11}	0.01556	8,32%
2.17398	8.88982×10^{-11}	0.01469	10,05%

2.12394	1.94658×10^{-10}	0.03217	10,38%
2.07391	3.73349×10^{-10}	0.06171	12,46%
1.92379	2.7546×10^{-11}	0.00455	16,05%
1.87375	6.15819×10^{-11}	0.01018	27,57%
1.82371	6.05516×10^{-11}	0.01001	10,49%
1.77366	4.52955×10^{-11}	0.00749	7,09%
1.72362	4.25037×10^{-11}	0.00703	5,23%
1.67357	3.92418×10^{-11}	0.00649	5,14%
1.62353	3.77306×10^{-11}	0.00624	6,22%
1.57349	3.52474×10^{-11}	0.00583	7,89%
1.52345	2.57287×10^{-11}	0.00425	9,46%
1.47341	9.86601×10^{-12}	0.00163	11,36%
1.43586	9.48367×10^{-13}	1.56755×10^{-4}	8,47%
1.41594	8.7008×10^{-13}	1.43815×10^{-4}	8,21%
1.40272	1.00591×10^{-10}	0.01663	7,79%
1.39185	2.06146×10^{-10}	0.03407	5,20%
1.38236	4.41721×10^{-11}	0.0073	5,00%
1.37371	3.24834×10^{-13}	5.36916×10^{-5}	5,00%
1.3653	1.2667×10^{-11}	0.00209	5,00%
1.35676	9.60549×10^{-15}	1.58768×10^{-6}	5,00%
1.34817	6.50422×10^{-12}	0.00108	5,00%
1.33979	1.59065×10^{-10}	0.02629	5,01%
1.33194	2.89657×10^{-10}	0.04788	5,00%
1.32481	2.13678×10^{-10}	0.03532	5,00%
1.31832	1.02477×10^{-10}	0.01694	5,00%
1.31233	1.3036×10^{-10}	0.02155	5,00%
1.3067	2.38472×10^{-12}	3.94169×10^{-4}	5,00%
1.3014	4.06079×10^{-12}	6.71205×10^{-4}	5,00%
1.29634	1.66593×10^{-12}	2.7536×10^{-4}	5,00%
1.29151	6.42193×10^{-13}	1.06148×10^{-4}	5,00%
1.2868	3.57863×10^{-12}	5.91509×10^{-4}	5,00%
1.28182	5.77764×10^{-11}	0.00955	5,00%
1.27588	3.90487×10^{-12}	6.45433×10^{-4}	5,00%
1.26908	1.07892×10^{-10}	0.01783	5,00%
1.25638	1.44518×10^{-10}	0.02389	5,00%
1.25098	8.65048×10^{-12}	0.00143	5,00%
1.246	1.05718×10^{-11}	0.00175	5,00%
1.24138	3.80166×10^{-12}	6.28373×10^{-4}	5,00%
1.23703	5.12212×10^{-13}	8.46631×10^{-4}	5,00%
1.23278	3.5404×10^{-12}	5.8519×10^{-4}	5,00%
1.22833	3.82275×10^{-11}	0.00632	5,00%

Table S7. Evolution of sodium concentrations for the NVMFP/C cathode during the discharging process, including the $D\times t\times L^{-2}$ kinetic condition and associated error bars.

xNa^+ in $Na_xV_{1.5}Fe_{0.25}Mn_{0.25}(PO_4)_3$	D	$D\times t\times L^{-2}$	Error bar

1.30105	7.90421×10^{-11}	0.01306	9,25%
1.35112	5.85686×10^{-11}	0.00968	5,48%
1.40118	6.95428×10^{-11}	0.01149	6,80%
1.45125	6.282×10^{-11}	0.01038	5,42%
1.50131	6.5541×10^{-11}	0.01083	5,23%
1.55136	7.07789×10^{-11}	0.0117	6,09%
1.60142	7.51885×10^{-11}	0.01243	6,74%
1.65148	8.23715×10^{-11}	0.01362	7,27%
1.70154	8.39555×10^{-11}	0.01388	7,34%
1.7516	8.86613×10^{-11}	0.01465	7,75%
1.80167	8.03509×10^{-11}	0.01328	7,18%
1.85173	7.25362×10^{-11}	0.01199	7,28%
1.90179	6.73229×10^{-11}	0.01113	6,89%
1.95185	6.20056×10^{-11}	0.01025	6,64%
2.00191	7.02612×10^{-11}	0.01161	7,54%
2.05197	6.20117×10^{-11}	0.01025	7,47%
2.10202	7.72839×10^{-11}	0.01277	9,08%
2.15208	7.85334×10^{-11}	0.01298	8,83%
2.20214	8.21264×10^{-11}	0.01357	10,48%
2.25221	7.57358×10^{-11}	0.01252	10,01%
2.30227	7.76654×10^{-11}	0.01284	9,65%
2.35233	7.28236×10^{-11}	0.01204	8,86%
2.4024	6.84081×10^{-11}	0.01131	9,23%
2.45246	6.90576×10^{-11}	0.01141	8,84%
2.50251	8.51438×10^{-11}	0.01407	9,21%
2.55257	9.67219×10^{-11}	0.01599	8,78%
2.60263	1.77516×10^{-10}	0.02934	7,55%
2.65269	1.80685×10^{-10}	0.02987	10,37%
2.70275	2.36704×10^{-10}	0.03912	11,89%
2.75281	2.58124×10^{-10}	0.04267	12,84%
2.80287	3.06445×10^{-10}	0.05065	14,74%
2.85293	4.71732×10^{-10}	0.07797	16,08%
2.95304	6.61303×10^{-11}	0.01093	30,01%
3.0031	1.35722×10^{-11}	0.00224	20,91%
3.05315	4.03351×10^{-11}	0.00667	6,77%
3.10321	1.55299×10^{-11}	0.00257	12,49%
3.15326	1.03235×10^{-11}	0.00171	6,02%
3.20331	3.67936×10^{-11}	0.00608	8,77%
3.25336	5.44934×10^{-10}	0.09007	24,38%
3.30341	7.73143×10^{-11}	0.01278	38,74%
3.35345	5.3449×10^{-10}	0.08835	37,08%
3.4035	2.51614×10^{-10}	0.04159	23,81%
3.45355	2.24705×10^{-10}	0.03714	7,61%
3.55364	5.61909×10^{-11}	0.00929	6,53%
3.60369	1.799×10^{-11}	0.00297	8,14%
3.65374	1.09699×10^{-11}	0.00181	9,30%

3.70378	9.15005×10^{-12}	0.00151	10,26%
3.75383	8.77843×10^{-12}	0.00145	8,41%
3.80388	8.58924×10^{-12}	0.00142	12,37%
3.85392	9.02145×10^{-12}	0.00149	10,99%
3.90397	9.60984×10^{-12}	0.00159	12,57%
3.95402	1.20296×10^{-11}	0.00199	13,75%
3.99351	5.79829×10^{-12}	9.58396×10^{-4}	17,31%
4.01844	3.49561×10^{-13}	5.77787×10^{-5}	18,87%
4.03885	1.96916×10^{-15}	3.2548×10^{-7}	15,15%
4.06047	1.38216×10^{-14}	2.28456×10^{-6}	14,96%
4.08493	3.81422×10^{-14}	6.3045×10^{-6}	19,10%
4.11009	2.01923×10^{-13}	3.33757×10^{-5}	20,46%
4.13331	3.17644×10^{-13}	5.25032×10^{-5}	20,37%
4.1536	1.77719×10^{-13}	2.9375×10^{-5}	18,35%
4.17149	9.36706×10^{-14}	1.54827×10^{-5}	14,45%
4.18767	9.03568×10^{-14}	1.4935×10^{-5}	17,33%
4.20217	2.81282×10^{-14}	4.64929×10^{-6}	14,90%
4.21514	9.74167×10^{-15}	1.61019×10^{-6}	8,05%
4.22711	1.41933×10^{-14}	2.34599×10^{-6}	5,19%
4.23808	1.12787×10^{-14}	1.86425×10^{-6}	5,08%
4.24859	5.00872×10^{-16}	8.27888×10^{-8}	5,85%
4.25928	7.00856×10^{-15}	1.15844×10^{-6}	5,10%

Table S8. Fitted EIS parameters of NVMFP/C.

Condition	R_o	CPE_{CEI}-T	CPE_{CEI}-P	R_{CEI}	CPE_{ct}-T	CPE_{ct}-P	R_{ct}	W_1-R	W_1-T	W_1-P
After 1st charge	5,704	$4{,}1538\times 10^{-5}$	0,75113	143,4	0,0012908	0,90695	2090	63485	6,482	0,81475
After 1st discharge	5.203	$8{,}7435\times 10^{-6}$	0,79586	550,2	0,00037396	0,70106	1462	156	10,33	0,70014

References

[1] W. Li, J. Li, R. Li, X. Li, J. Gao, S.M. Hao, W. Zhou, Study on sodium storage properties of manganese-doped sodium vanadium phosphate cathode materials, Batter. Energy. 2 (2023) 1–11. https://doi.org/10.1002/bte2.20220042.

[2] C. Xu, R. Xiao, J. Zhao, F. Ding, Y. Yang, X. Rong, X. Guo, C. Yang, H. Liu, B. Zhong, Y.S. Hu, Mn-Rich Phosphate Cathodes for Na-Ion Batteries with Superior Rate Performance, ACS Energy Lett. 7 (2022) 97–107. https://doi.org/10.1021/acsenergylett.1c02107.

[3] J. Zhang, X. Zhao, Y. Song, Q. Li, Y. Liu, J. Chen, X. Xing, Understanding the superior sodium-ion storage in a novel Na3.5Mn0.5V1.5(PO4)3 cathode, Energy Storage Mater. 23 (2019) 25–34. https://doi.org/10.1016/j.ensm.2019.05.041.

[4] F. Lu, Y. Lu, L. Zhao, Dual carbon decorated Na3.5Mn0.5V1.5(PO4)3 cathode with high-density and long-cycling span-life for sodium-ion batteries, J. Power Sources. 645 (2025) 237194. https://doi.org/10.1016/j.jpowsour.2025.237194.

[5] Y. Fan, Z. Peng, J. He, N. Sun, F. Ma, T. Zhang, F. Zhang, Simultaneous modification of Na+-rich and Mn2+-doping on Na3V2(PO4)3 for superior electrochemical performance: Experimental and theoretical study, J. Alloys Compd. 1010 (2025) 177407.

https://doi.org/10.1016/j.jallcom.2024.177407.

[6] M.T. Ahsan, Z. Wu, Y. Liu, H. Chen, M. Li, D. Li, Unlocking the Ultrastable Sodium Storage via Cation Engineering in Vanadium-Iron-Based NASICON Framework, Adv. Energy Mater. 04885 (2025) 1–12. https://doi.org/10.1002/aenm.202504885.

[7] Y. Chen, Q. Li, P. Wang, X. Liao, J. Chen, X. Zhang, Q. Zheng, D. Lin, K. Lam, High-Energy-Density Cathode Achieved via the Activation of a Three-Electron Reaction in Sodium Manganese Vanadium Phosphate for Sodium-Ion Batteries, Small. 2 (2023) 3–11. https://doi.org/10.1002/smll.202304002.

[8] X. Zhang, H. Mao, Z. Chen, L. Zhou, L. Liu, M. Wu, Z. Lv, Z. Zhang, Y. Zhong, Y.-S. Hu, Rational Design of Phosphate Cathodes with Improved Na-storage Performance, ACS Energy Lett. 10 (2025) 2804–2810. https://doi.org/10.1021/ACSENERGYLETT.5C00653.

[9] Y. Zhu, H. Xu, Y. Bao, S. Li, Y. Chen, Ternary NASICON-Type Na3.25VMn0.25Fe0.75(PO4)3/NC@CNTs Cathode with Reversible Multielectron Reaction and Long Life for Na-Ion Batteries, ACS Appl. Mater. Interfaces. 17 (2025) 7581–7594. https://doi.org/10.1021/acsami.4c15767.

[10] C. Xu, J. Zhao, E. Wang, X. Liu, X. Shen, X. Rong, Q. Zheng, G. Ren, N. Zhang, X. Liu, X. Guo, C. Yang, H. Liu, B. Zhong, Y.S. Hu, A Novel NASICON-Typed Na4VMn0.5Fe0.5(PO4)3 Cathode for High-Performance Na-Ion Batteries, Adv. Energy Mater. 11 (2021) 1–9. https://doi.org/10.1002/aenm.202100729.

[11] P.X. Xie, Q.Y. Zhao, H. Dong, T. Long, M.S. Ding, B. Xie, X.F. Wang, W. Ling, M. Liu, X.W. Wu, P.F. Wang, X.X. Zeng, Reversible V4+/V5+ redox in Na4VFe(PO4)3 cathode for high-power sodium-ion batteries, Chem. Eng. J. 509 (2025) 161209. https://doi.org/10.1016/j.cej.2025.161209.